Coherence expansion and polariton condensate formation in a semiconductor microcavity

V.V. Belykh,[1,*] N.N. Sibeldin,[1] V.D. Kulakovskii,[2] M.M. Glazov,[3]
M.A. Semina,[3] C. Schneider,[4] S. Höfling,[4] M. Kamp,[4] and A. Forchel[4]

[1] *P.N. Lebedev Physical Institute, Russian Academy of Sciences, Moscow, 119991 Russia*
[2] *Institute of Solid State Physics, Russian Academy of Sciences, Chernogolovka, 142432 Russia*
[3] *Ioffe Physical-Technical Institute of the Russian Academy of Sciences, St. Petersburg, 194021 Russia*
[4] *Technische Physik, Physikalisches Institut and Wilhelm Conrad Röntgen Research Center for Complex Material Systems, Universität Würzburg, D-97074 Würzburg, Germany*

The dynamics of the first order spatial coherence, $g^{(1)}$, for a polariton system in a high-Q GaAs microcavity was investigated on the basis of Young's double slit experiment under 3 ps pulse excitation at the conditions of polariton Bose-Einstein condensation. It was found that in the process of condensate formation, the coherence buildup time increases almost linearly with the distance indicating that the coherence expands with almost constant velocity of about 10^8 cm/s. The coherence is strongly affected by exciton reservoir and polariton decay kinetics. It is smaller than coherence in thermally equilibrium system during the growth of condensate density and well exceeds it at the end of condensate decay.

One of the most important characteristics of Bose-Einstein condensate is the spatial coherence or the off-diagonal long range order, i.e. the property of the system to share the same wave function at different points separated by a distance larger than the thermal de Broglie wavelength. To understand the processes governing the Bose-Einstein condensation (BEC), it is important to know how fast the coherence is established throughout the system during the condensate formation. This question was addressed theoretically in Refs. [1, 2], where it was shown that in the process of a condensation particles first relax to the low energy or so-called coherent region where the kinetic energy of the particle is of the order of its interaction energy with other particles. Second, the fluctuations of density are smoothed out and a "quasicondensate" is formed. Further, the phase fluctuations disappear resulting in the long range order formation within the system signifying the onset of the "true condensate". The timescales of these processes are quite different: the relaxation to the low energy region is mainly determined by the stimulated scattering processes, whereas the quasicondensate formation is governed by the interparticle interactions. Experimentally, the dynamics of spatial coherence formation was first studied for a gas of ultracold atoms in Ref. [3], where it was found that the coherence expands with a constant velocity of about 0.1 mm/s.

In this Letter we discuss the expansion of the spatial coherence in a condensate of mixed exciton-photon states, polaritons, in a semiconductor microcavity (MC) with embedded quantum wells. The bosonic statistics of these particles and the extremely light effective mass m ($\sim 10^{-5}$ of the free electron mass m_e) allow one to observe MC polariton BEC up to the room temperatures, which inspired a considerable attention to this system in the last decade. After the first experimental demonstration of MC polariton BEC [4] a number of related phenomena in the MC polariton system have been observed and discussed: superfluidity [5], quantized vortices [6], spin-Meissner effect [7] and Josephson effect [8] (see [9] for a review). Compared with atomic BEC, the MC polariton condensation is highly specific: the system of MC polaritons is strongly nonequilibrium due to the short lifetime of the quasiparticles and the presence of pumping [10].

The first order spatial coherence function, $g^{(1)}$, is related to the off-diagonal elements of the coordinate dependent polariton density matrix $\varrho(\boldsymbol{\rho}, \boldsymbol{\rho'})$ as

$$g^{(1)}(\boldsymbol{\rho}) = \frac{\varrho(\boldsymbol{\rho}, 0)}{\sqrt{\varrho(\boldsymbol{\rho}, \boldsymbol{\rho})\varrho(0, 0)}}, \qquad (1)$$

and can be probed in the MC polariton system by measuring the interference of the light emitted from different points on the sample [4, 11, 12]. Dynamics of $g^{(1)}$ in a process of MC polariton condensate formation was studied experimentally using a Michelson interferometer in [13] in a CdTe-based MC for the fixed separation between condensate regions $\Delta x = 8.5$ μm and very recently in [14] in a GaAs-based MC, where the temporal dynamics of $g^{(1)}$ was related with the transition from photon to polariton lasing. A systematic study of spatial-temporal coherence expansion in a process of condensate formation is still missing to the best of our knowledge.

In the present work we study the spatial coherence dynamics of the polariton system in a high-Q GaAs-based MC in the geometry of Young's double-slit experiment [11] for different separations between the slits under pulsed excitation. This allows us to trace the dependence $g^{(1)}(\Delta x)$ at different times and extract the dynamics of the coherence length r_c. Maximum $r_c \approx 17$ μm is reached approximately simultaneously with the maximal ground state population, at the excitation density P not strongly exceeding threshold density P_{thr} and r_c decreases with P at $P \gg P_{thr}$. We have found that the coherence buildup time grows almost linearly with

distance Δx, that is the coherence expands with almost constant velocity. We show that formation of the spatial coherence under pulsed excitation with $P < 2P_{thr}$ is governed by the processes of polariton relaxation towards the ground state, whereas amplitude and phase fluctuations of the quasicondensate are not suppressed in MC polariton system.

The sample is a half wavelength MC with Bragg reflectors made of 32 (for the top mirror) and 36 (for the bottom mirror) AlAs and $Al_{0.13}Ga_{0.87}As$ pairs. It has a Q-factor of about 7000 and the Rabi splitting of 5 meV. All the experiments were performed at 10 K and photon-exciton detuning of -9 meV. The sample was excited by the linearly polarized radiation of a mode-locked Ti-sapphire laser generating a periodic train of 2.5-ps-long pulses at a repetition rate of 76 MHz. The angle of incidence of the excitation laser beam was 60^0 with respect to the sample normal and the excitation photon energy corresponded to the reflection minimum of the mirror at this angle and was 11 meV above the energy of the bare exciton. The beam was focused in a 20 μm spot on the sample surface. The spot was imaged with magnification of $\Gamma = 6$ on the light-absorbing plate with two transparent parallel slits. The interference pattern of the emission coming from the regions of the sample selected by the two slits was formed on the Hamamatsu streak camera slit, like in Ref. [11]. Different slits pairs with separations X between slits in each pair ranging from 20 to 160 μm and slit width 5 μm was used to study $g^{(1)}(\Delta x)$, where $\Delta x = X/\Gamma$. Spatial coherence $g^{(1)}$ was extracted as the visibility of the interference pattern $g^{(1)} = (I_{max} - I_{min})/(I_{max} + I_{min})$, where I_{min} and I_{max} are minimal and maximal intensities within one period of interference pattern, averaged over all the observed periods. The time resolution in this case was 3 ps. To study the energy-time dynamics of the MC emission it was dispersed by a spectrometer coupled to the streak camera. In this configuration spectral and temporal resolutions were 0.25 meV and 20 ps, respectively.

To convert the intensity $I(t)$, measured by the streak-camera to the number of polaritons N at states with wavevectors $|k| < 3$ μm^{-1}, corresponding to the collection aperture (above BEC threshold they mainly concentrated at $k \approx 0$), the integrated intensity of the MC photoluminescence (PL) I_{PL} was measured by the sensitive power meter. Then the number of emitted photons per laser pulse N_{pulse} was evaluated by the relation $N_{pulse} = 2I_{PL}/(f\hbar\omega)$, where factor 2 takes into account two directions of photon emission, f is the laser pulse repetition rate and $\hbar\omega$ is the energy of emitted photons. Finally, the number of polaritons was evaluated by the relation $N(t) = N_{pulse}\tau_{LP}I(t)/\int I(t)dt$, where $\tau_{LP} = \tau_C/|C|^2 \approx 3$ ps is the polariton lifetime at the bottom of the lower polariton (LP) branch (C is the photon Hopfield coefficient, τ_C is the lifetime of photon in a cavity, which was determined from the linewidth γ_C of strongly photonlike polariton: $\tau_C = \hbar/\gamma_C$).

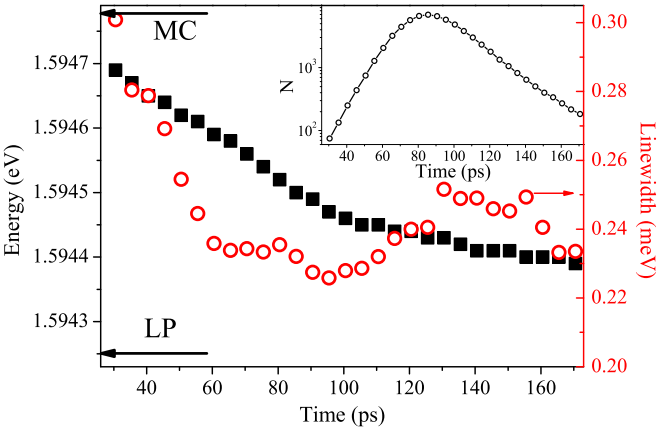

FIG. 1: Dynamics of the energy (full squares, left axis) and FWHM (empty circles, right axis) of the LP emission line. E_{MC} and E_{LP} are marked by black arrows. Inset shows the number of LPs near $k = 0$. Excitation power is $1.8P_{thr}$.

At low excitation density P the PL dynamics of the LP branch is relatively slow, and the angular distribution of intensity indicates a bottleneck effect. As P is increased above the BEC threshold $P_{thr} = 0.7$ kW/cm^2 (this value corresponds to the time-averaged power of pulsed excitation), a fast and intense component in the PL dynamics corresponding to $k \approx 0$ appears. Onset of the fast component is accompanied by the blueshift of the spectral line and decrease of its width, which becomes determined by the spectral resolution (Fig. 1). The energy position of the spectral line is close the bare MC mode E_{MC} just after the excitation pulse and relaxes to the energy of LP mode at low particle density E_{LP} with time. The maximum population (inset in Fig. 1) is reached when the spectral line energy is between the MC and LP modes indicating that BEC is observed in the strong coupling regime despite the high particle density [15–17].

Below P_{thr} interference fringes in the double slit experiment are observed only for the smallest studied slits separation, and $g^{(1)}(\Delta x = 3$ μm$)$ at $0.9P_{thr}$ is less than 0.3. Above P_{thr} the interference fringes are well resolved up to $\Delta x = 20$ μm. Figure 2(a) shows the time dynamics of the interference of the emission coming from the sample regions separated by $\Delta x = 3$ and 17 μm.

The dynamics of the spatial coherence $g^{(1)}$ for different separations Δx at $P = 1.8P_{thr}$ is presented in Fig. 2(b) together with the dynamics of the polariton number N at the bottom of the LP branch. Figure 2(b) shows that the maximum value of $g^{(1)}$ decreases with increased Δx and the decay of $g^{(1)}$ in the whole range of Δx occurs much slower than that of the condensate density.

Interestingly, Fig. 2(b) shows that the coherence buildup time increases with an increase of Δx, indicating a finite velocity of coherence expansion. We define the

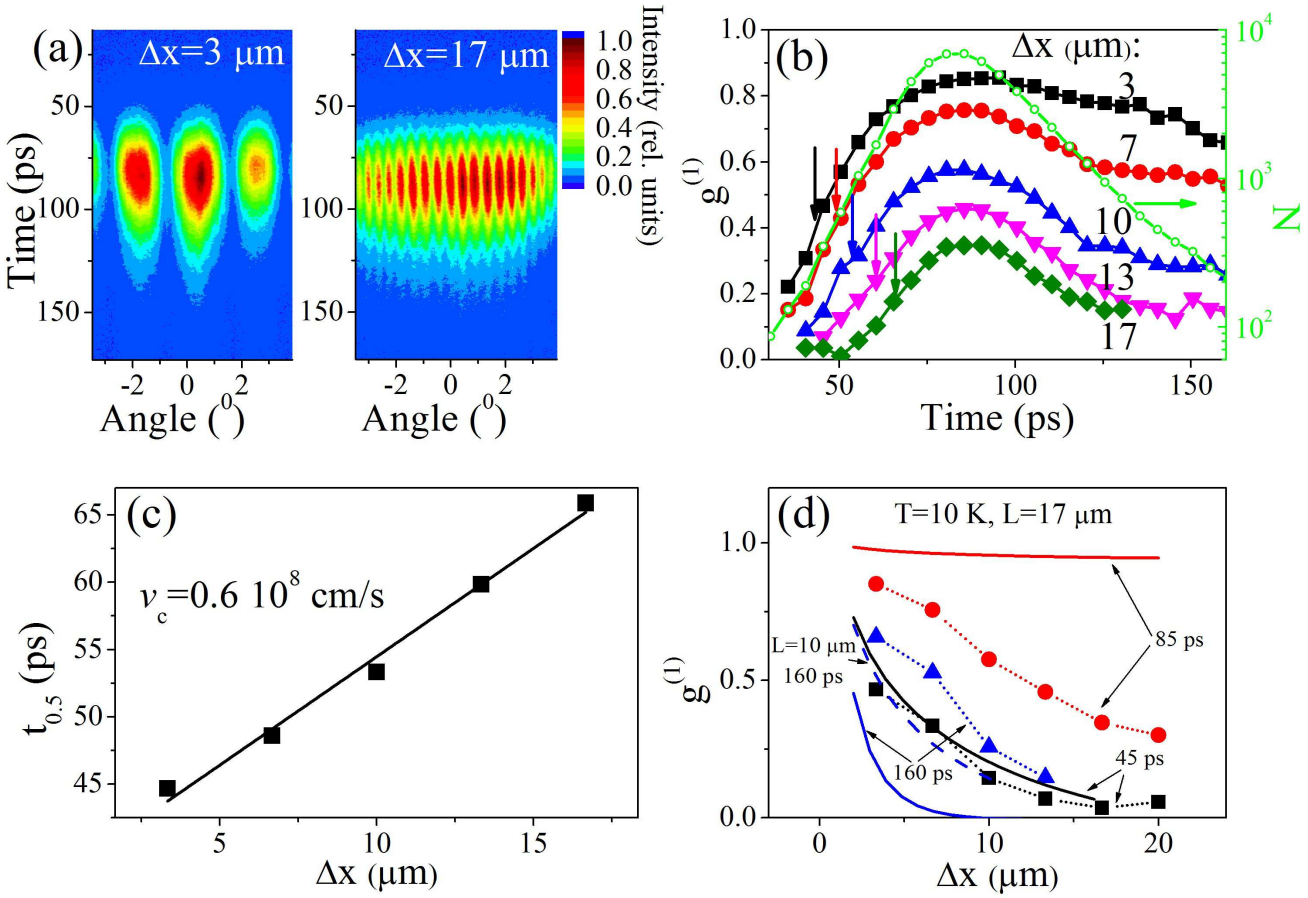

FIG. 2: (a) Streak camera images of the interference patterns of the emission coming from regions of the sample separated by $\Delta x = 3$ and 17 μm. Horizontal axis corresponds to the angle of the emission passed through the slits with respect to the sample normal. (b) Dynamics of the spatial coherence for different Δx (left axis) and number of particles near the bottom of the LP branch (right axis). Arrows mark the times $t_{0.5}$, when $g^{(1)}$ reaches half of its maximal value. (c) Dependence of the coherence buildup time $t_{0.5}$ on Δx. Solid curve shows linear fit. The slope of the dependence yields the coherence expansion velocity v_c. (d) Dependences of spatial coherence function on Δx at different times t. Experimental results are shown by symbols, solid lines show dependences calculated at the same times as experimental ones for the condensate size $L = 17$ μm and dashed line is dependence calculated at $t = 160$ ps and $L = 10$ μm. Excitation power is $1.8P_{thr}$.

coherence buildup time $t_{0.5}(\Delta x)$ as the time when $g^{(1)}$ reaches half of its maximum value for a given Δx. These times are marked by arrows in Fig. 2(b). Figure 2(c) shows that the dependence of $t_{0.5}$ on Δx is close to linear indicating that the coherence expands with almost constant velocity $v_c = 0.6 \cdot 10^8$ cm/s.

Figure 3 shows the coherence length r_c, which is defined from $g^{(1)}(r_c) = 1/e$ and number of polaritons at the bottom of the LP branch N for $P > P_{thr}$. At the beginning of the BEC, r_c grows almost linearly with time, reaches its maximum and decays afterwards. It follows from Fig. 3, that r_c and N reach their maximal values almost at the same time, but the decay of N at high P occurs much faster than that of r_c: after $\sim$ 30 ps of relatively fast decay, in the dynamics of r_c appears a slow component preserving the value of r_c at the level 0.5...0.8 from its maximal value for several tens of picoseconds in the range where N decreases by more than an order of magnitude. Furthermore, Fig. 3 shows that the buildup of the coherence at $P = 1.2P_{thr}$ begins when the particle number N is more than one order of magnitude smaller than that at $P = 4.2P_{thr}$ and that the maximal value of r_c decreases with P at $P > 2P_{thr}$ in spite of a strong (about an two orders of magnitude) increase of the condensate density. These facts show that the length of coherence, as well as the rate of its increase, is not solely defined by the condensate occupation because of the nonequilibrium nature of the polariton BEC.

In a 2D system of a finite size L under the conditions of thermal equilibrium the number of particles in the ground state can be estimated as

$$N_0 = N - N', \qquad (2)$$

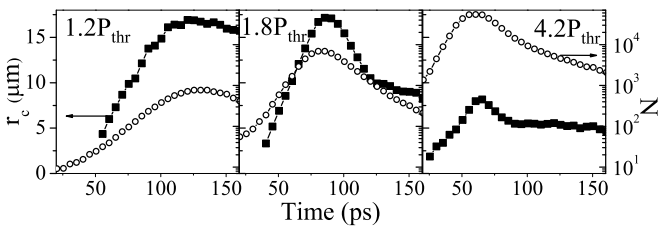

FIG. 3: Dynamics of the coherence length (full squares, left axes, linear scales) and number of particles near the bottom of the LP branch (empty circles, right axes, logarithmic scales) at different excitation powers.

where N is the total number of polaritons (neglecting those in the reservoir), N' is the number of polaritons in all states but the ground,

$$N' = \int_{1/L}^{\infty} \frac{kdkL^2}{\pi} (e^{\frac{\hbar^2 k^2}{2mT}} - 1)^{-1}, \qquad (3)$$

where T is the temperature measured in the units of energy. It is assumed in Eq. (3), that the chemical potential $\mu = 0$. It follows from Figs. 2(b) and 3 that the onset of spatial coherence at $P < 2P_{thr}$ starts at $N \sim 10^2$. This value is less than the estimated from Eq. (3) $N \approx 400$ at $T = 10$ K in the investigated LP system with the lateral size $L \approx 17$ μm and $m = 5 \cdot 10^{-5} m_e$. Thus, the formation of spatial coherence starts at negative chemical potential μ and hence governed by the relaxation process of polaritons to the low energy region, while interaction-induced suppression of amplitude and phase fluctuations plays no role [1, 2]. We note also, that at $P < 2P_{thr}$ the estimated value of the interaction energy for the condensed polaritons $\Delta E = \alpha N_0 / L^2 < 2$ μeV (where $\alpha = 10^{-12}$ meVcm^2 is the polariton-polariton interaction constant) is much less than thermal energy $T \approx 1$ meV. Hence, $g^{(1)}$ should be close to that for the classical noninteracting gas with the particle distribution function N_k [11]:

$$g^{(1)}(\Delta x) = \frac{\frac{L^2}{\pi} \int_{1/L}^{\infty} J_0(\Delta x k) N_k k dk + N_0}{\frac{L^2}{\pi} \int_{1/L}^{\infty} N_k k dk + N_0}, \qquad (4)$$

where $J_0(x)$ is the zero order Bessel function.

The detailed modeling of the polariton distribution similar to that in Refs. [18] is beyond the scope of the present paper. Here we compare the experimental dependences $g^{(1)}(\Delta x)$ with ones calculated for the thermal Bose distribution of the polaritons with the use of $T = 10$ K and the value of and chemical potential determined from the measured polariton number N in the low energy region. In the range of growing N this simulation gives an upper limit for $g^{(1)}$, as the density of polaritons in excited states should exceed the equilibrium one, in order to provide the income of polaritons to the ground state.

The results of calculation for three different stages: condensation onset, maximum condensate density and its decay, are shown in Fig. 2(d) for $P = 1.8P_{thr}$ and the condensate size $L = 17$ μm determined from the experiment. It is seen that the experimental dependence $g^{(1)}(\Delta x)$ is slightly below the calculated thermally equilibrium one in the first stage ($t = 45$ ps), the difference strongly increases in the second stage ($t = 85$ ps) whereas in the third stage ($t = 160$ ps) experimental values $g^{(1)}(\Delta x)$ turn out well above the calculated ones. The letter is especially surprising as it is difficult to expect the effective polariton temperature can be smaller than the bath temperature in the range of condensate decay. Measurements of polariton population along the LP branch (not shown) indicate that the distribution function approaches thermal one at the onset of condensation, but the occupation numbers of low $k \neq 0$ states are slightly increased compared to thermal values, which explains a small discrepancy between the experimental and calculated $g^{(1)}(\Delta x)$ at $t = 45$ ps when $N \approx 350 < N'$.

An increase in the discrepancy between the experimental and calculated $g^{(1)}(\Delta x)$ in the range of maximum N at $t = 85$ ps when $N \approx 7000 \gg N'$ indicates that the polariton system becomes more nonequilibrium at high condensate density. The most probable reason for that is the runaway of condensed polaritons from the small bounded (~ 20 μm) photoexcited region due to their repulsive interaction with a dense exciton reservoir [19]. In addition, for equilibrium system with $N_0 \gg N'$, the coherence is defined by the amplitude and phase fluctuations of the ground state wavefunction not taken into account in Eq. (4). Indeed, the quasicondensate amplitude fluctuations are suppressed during the time $\tau_A \approx \hbar L^2/(\alpha N)$ [1, 2], determined by the interparticle interaction. Taking $\alpha = 10^{-12}$ meVcm^2, $N = 7000$, $L = 17$ μm we obtain value $\tau_A \sim 0.3$ ns that exceeds the lifetime of polariton condensate at $P = 1.8P_{thr}$, which is about 100 ps (Fig. 3). While amplitude fluctuations and especially phase fluctuations are not suppressed in our experiment, the coherence length is determined by the healing length $\xi = \frac{\hbar L}{\sqrt{2m\alpha N}}$ [1, 2], which is about 20 μm at $P = 1.8P_{thr}$ ($N \approx 7000$) and decreases up to 10 μm at $P = 4.2P_{thr}$ due to increased N (Fig. 3).

Finally, let us discuss the reason for the unexpectedly high coherence in the decaying polariton system at $t \sim 160$ ps with $N \approx 200 < N'$ which exceeds markedly the coherence in the thermally equilibrium system. Note that the calculations underestimate experimental values of $g^{(1)}$ even if one takes unrealistically small condensate size $L = 10$ μm (dashed line in Fig. 2d). At large $t > 100$ ps the reservoir becomes highly depleted, and the equilibrium in the system is established mainly via rather ineffective excitation of condensed polaritons by acoustic phonons with characteristic time exceeding the intensity decay time τ. In this case the wave function at a given distance $\boldsymbol{\rho}$ decays as $\psi(\boldsymbol{\rho}) \propto \exp(-\frac{t}{2\tau})$. It fol-

lows then, that both diagonal and off-diagonal elements of the polariton density matrix decay approximately with the same rate $1/\tau$ resulting in a nearly constant ratio of the polariton numbers in the ground state to that in the excited states well exceeding the decaying equilibrium ratio at long times. As a result $g^{(1)}$ weakly decreases with time even in the range where $N < N'$, see Eq. (1), in agreement with the experiment.

To conclude, we have studied the dynamics of the spatial coherence for a condensate of MC polaritons under pulsed ps-long excitation for different excitation powers. It has been found that in the process of condensate formation, first order coherence expands with almost constant velocity of about 10^8 cm/s. We have shown that the coherence is determined not only by the density of low-k polaritons, but also by the reservoir population. The coherence length r_c and the number of low-k polaritons N reach their maximal values almost simultaneously, afterwards r_c decays much slower than N. We have demonstrated that the onset of spatial coherence is determined by the narrowing of polariton distribution in k-space rather than formation of the condensate phase, and at high excitation density coherence is limited by condensate amplitude fluctuations. The true condensate i.e. macroscopic occupation of the ground state with suppressed phase fluctuation is not achieved under ps-long pulsed pumping.

We are grateful to D.A. Mylnikov for help in the experiment and S.S. Gavrilov, N.N. Gippius, L.V. Keldysh, A.V. Sekretenko, S.G. Tikhodeev and V.B. Timofeev for valuable advice and useful discussions. This study was supported by the Russian Foundation for Basic Research (projects no. 11-02-01310, 11-02-12261, 11-02-00573) and the Presidium of the Russian Academy of Sciences (Programs for Fundamental Research). MMG is grateful to EU project POLAPHEN for partial support. MAS was partially supported by the RF President Grant NSh-2901.2012.2.

* Electronic address: belykh@lebedev.ru

[1] Yu.M. Kagan, B.V. Svistunov, and G.V. Shlyapnikov, JETP **75**, 387 (1992).
[2] Yu. Kagan and B.V. Svistunov, JETP **78**, 187 (1994).
[3] S. Ritter et al., Phys. Rev. Lett. **98**, 090402 (2007).
[4] J. Kasprzak *et al.*, Nature **443**, 409 (2006).
[5] A. Amo *et al.*, Nature Phys. **5**, 805 (2009).
[6] K. G. Lagoudakis *et al.*, Nature Phys. **4**, 706 (2008).
[7] A. V. Larionov *et al.*, Phys. Rev. Lett. **105**, 256401 (2010).
[8] K. G. Lagoudakis *et al.*, Phys. Rev. Lett. **105**, 120403 (2010).
[9] D. Sanvitto and V. Timofeev (editors), *Exciton Polaritons in Microcavities* (Springer, New York, 2012), Springer Series in solid-state sciences Vol. 172.
[10] F. Tassone *et al.*, Phys. Rev. B **56**, 7554 (1997).
[11] H. Deng *et al.*, Phys. Rev. Lett. **99**, 126403 (2007).
[12] G. Roumpos *et al.*, PNAS **109**, 6467 (2012).
[13] G. Nardin *et al.*, Phys. Rev. Lett. **103**, 256402 (2009).
[14] H. Ohadi *et al.*, Phys. Rev. Lett. **109**, 016404 (2012).
[15] J. Keeling *et al.*, Phys. Rev. B **72**, 115320 (2005).
[16] K. Kamide and T. Ogawa, Phys. Rev. Lett. **105**, 056401 (2010).
[17] T. Byrnes *et al.*, Phys. Rev. Lett. **105**, 186402 (2010).
[18] G. Malpuech *et al.*, Semicond. Sci. Technol. **18**, S395 (2003); D. Sarchi and V. Savona, Phys. Rev. B **75**, 115326 (2007); T. D. Doan *et al.*, Phys. Rev. B **78**, 205306 (2008).
[19] A.S. Brichkin *et al.*, Phys. Rev. B **84**, 195301 (2011).